Flow field-flow fractionation with off-line electrothermal atomic absorption spectrometry for size characterization of silver nanoparticles

Kanchana Songsilawat, Juwadee Shiowatana, Atitaya Siripinyanond*

Department of Chemistry and Center for Innovation in Chemistry, Faculty of Science, Mahidol University, Rama VI Rd., Bangkok 10400, Thailand

ARTICLE INFO

ABSTRACT

Flow field-flow fractionation (Fl-FFF) with off-line electrothermal atomic absorption spectrometry (ETAAS) detection was developed and employed for particle size characterization of Ag NPs stabilized by citrate, pectin, and alginate. Citrate stabilized-Ag NPs were prepared from sodium borohydride reduction of silver nitrate. Sodium citrate was used as the capping agent to stabilize Ag NPs and prevent the aggregation process. Pectin stabilized- and alginate stabilized-Ag NPs were prepared from ascorbic acid reduction of silver nitrate. Pectin and alginate were used as the capping agent for pectin stabilized- and alginate stabilized-Ag NPs, respectively. Three types of Ag NPs were characterized by using FlFFF, zeta potentiometer, and TEM technique. The mean particle sizes of Ag NPs as characterized by FlFFF were 9 nm, 19 nm, and 45 nm for citrate stabilized-, pectin stabilized-, and alginate stabilized-Ag NPs, respectively, in deionized water. Further, FlFFF with ETAAS detection was employed to observe the aggregation of Ag NPs of various types in environmental water in the absence and presence of humic acid. Citrate stabilized-Ag NPs underwent aggregation more rapid than the pectin stabilized- and alginate stabilized-Ag NPs as the latter two types were sterically stabilized. Further, humic acid could prolong the stability of Ag NPs in the environment.

© 2010 Elsevier B.V. All rights reserved.

1. Introduction

Silver nanoparticles (Ag NPs) are one of common engineered nanoparticles (ENPs) with at least one dimension within the size from approximately 1 nm to 100 nm [1]. Owing to their antibacterial properties, Ag NPs have been used in various consumer products including textiles, personal care products, food storage containers, and laundry additives. The release of Ag NPs into water and their mobilities in water should therefore be investigated. Silver ions (Ag^+) can be released from consumer products by oxidation of metallic silver (Ag^0) in contact with water [2,3]. Blaser et al. studied the model of total silver in the form of Ag^+ ions or AgNPs released from plastic and textile into water and indicated that up to 15% of the total Ag discharged into the environment [4]. Moreover, recent studies by Benn and Westerhoff confirmed that Ag NPs were easily released from nanosilver-coated socks during the washing process [5].

Recently, the issue of mobility and toxicity of Ag NPs has gained significant attention. In general, the smaller size can transport faster and has much higher toxicity than the larger size. Moreover, smaller size Ag NPs (<5 nm) are more toxic than any other forms of silver [6]. The aggregation is also one of the primary controls on

both transport and toxicity of Ag NPs in the aquatic environment. Not only temperature, pH, ionic strength of environmental water, and concentration of Ag NPs show significant effect on the aggregation process, but also the surface property of Ag NPs is important [7]. The surface property of Ag NPs depends on how Ag NPs are synthesized. Ag NPs can be synthesized using various methods resulting in different shapes, sizes, and surface properties for numerous applications [8]. Normally, Ag NPs are synthesized via reduction of silver nitrate in water using reductants and stabilizing agent or capping agent for control of particle size to ensure a stable suspension [9,10]. The reductant and stabilizing agents commonly used are sodium borohydride and sodium citrate, respectively. Greener processes for the production of greener nanomaterials were reported by use of nontoxic chemicals [11].

As the particle size of Ag NPs plays important roles to their mobility and hence toxicity, particle size characterization of Ag NPs is necessary. Size characterization techniques for Ag NPs include dynamic light scattering (DLS) [12], transmission electron microscopy (TEM) [7,13], atomic force microscopy (AMF) [14], size exclusion chromatography (SEC) [15], hydrodynamic chromatography (HDC) [15], and flow field-flow fractionation (FlFFF) [13]. The use of FlFFF coupled off-line with AFM to observe the structure of the smaller size fraction of aquatic colloids was reported to fractionate citrate-stabilized Ag NPs at environmentally relevant conditions [14]. In this study, the use of ETAAS as an off-line detector for the Ag NPs fractionated by FlFFF was evaluated. FlFFF with

---

* Corresponding author. Tel.: +66 2 201 5195; fax: +66 2 354 7151.
  E-mail address: scasp@mahidol.ac.th (A. Siripinyanond).

ETAAS detection was employed for size characterization of Ag NPs in environmental water. The aggregation phenomenon of Ag NPs from different synthesis methods including common method (citrate stabilized) and green synthesis (polysaccharide stabilized) in various types of water was investigated. The effect of humic acid on the aggregation of Ag NPs was also examined.

2. Experimental

2.1. Chemicals and samples

Silver nitrate was purchased from Carlo Erba (Rodano, MI, Italy). Sodium borohydride, sodium hydroxide, and sodium azide were purchased from Merck (Darmstadt, Germany). Humic acid and sodium citrate tribasic dihydrate were purchased from Sigma–Aldrich (Steinheim, Germany). Pectin and alginate were from Fluka (Buchs, Switzerland). Gold nanoparticle standard (Au NPs) of 10 nm diameter (Sigma–Aldrich) was used to calibrate the FlFFF channel. The humic acid stock solution (2000 mg L^{-1}) was made by dissolving 0.050 g of humic acid in 25 mL of deionized water.

Water samples were collected from three different sites including sea water from the Jausumran beach (Phetchaburi, Thailand), ground water from the Lopburi farm (Lopburi, Thailand), and tap water (Bangkok, Thailand). The samples were stored in a refrigerator and filtered through 0.45 μm membrane filters before use.

2.2. Silver nanoparticles synthesis

Citrate stabilized-Ag NPs were prepared as described previously by Yang et al. [16]. Briefly, 100 mL of 0.3 M silver nitrate and 8 mL of 12.6 M sodium citrate were mixed together in a conical flask, and then stirred at 50 rpm. Stirring was continued and 2 mL of 37 mM NaBH$_4$ was added into solution. The yellow solution was then observed.

For polysaccharide stabilized-Ag NPs, Ag NPs were prepared by the reduction of silver ion using ascorbic acid. Polysaccharide, i.e., pectin and alginate, were used to stabilize nanoparticles. Briefly, 100 mL of 0.1% (w/v) polysaccharide solution (pectin or alginate) were mixed together with freshly prepared ascorbic acid of 1 mM (50 mL) and vigorously stirred. Fifty milliliters of 2 mM silver nitrate solution was added into the solution and 0.3 M NaOH (0.1 mL) was added quickly. Stirring was continued and the final yellow solution was observed.

2.3. Instrumentation

The FlFFF system is a PN-1201-FO model (Postnova Analytics, Landsberg, Germany). The FlFFF channel dimensions are 27.7 cm length, 2.0 cm wide, and 254 μm thick. A 1-kDa regenerated cellulose membrane (Postnova) was used. The carrier liquid was 0.02% FL-70 and 0.02% NaN$_3$ was diluted in deionized water and adjusted to pH 9.2–10. Sample volume of 20 μL was introduced into FlFFF via the Rheodyne injector valve. A high pressure liquid chromatography (HPLC) pump (Model PN 2101, Postnova Analytics, Germany) was used to deliver the channel flow at 1 mL min^{-1}. The cross flow rate fixed at 1 mL min^{-1} was delivered by another HPLC pump of the same model. After fractionation, the effluent was directed through a UV detector (Model S3210 UV–visible detector; Postnova Analytics) and the detector was set at 400 nm for detection of the Ag NPs. The automatic fraction collector (Waters, Milford, MA, USA) was used to collect fraction from UV detector outlet. The FlFFF operating conditions are shown in Table 1.

A Perkin Elmer Model AAnalyst 100 (Norwalk, CT, USA) with deuterium background corrector was used for detection of silver after the UV absorption detector. The Perkin Elmer Model AS-72

Table 1
FlFFF operating condition.

FlFFF: Model PN-1021-FO	
Channel dimension/cm × cm × cm	27.7 long × 2.0 wide × 0.02 thick
Carrier liquid	0.02% FL-70 and 0.02 NaN$_3$ (pH 9.5)
Channel flow rate/mL min^{-1}	1.0
Cross flow rate/mL min^{-1}	1.0
Equilibration time/min	2.2
Membrane	1 kDa MWCO poly(regenerated cellulose acetate)

Table 2
Electrothermal atomic absorption spectrometer operating condition for silver detection.

ETAAS: Perkin Elmer Analyst 100-HGA-800				
Step		Temperature (°C)	Ramp time (s)	Hold time (s)
1	Drying	130	20	30
2	Ashing	800	20	30
3	Atomization	1800	0	8
4	Clean up	2600	1	5

autosampler was used to introduce solution into a graphite tube. The furnace operating condition for silver and silver nanoparticles measurement is summarized in Table 2.

The UV–visible absorption spectra of Ag NPs were observed by using UV–visible spectrophotometer (Model V-530, Jasco, Easton, MD, USA). Zeta potential measurements were carried out using the Zetasizer Nano ZS (Malvern Instruments Zetasizer1000 Hs, Malvern, UK). A transmission electron microscope (TEM), JEOL JEM-1230 (Peabody, MA, USA), was used to acquire images of the Ag NPs. The TEM was operated at 25 °C and 80 kV.

3. Results and discussion

3.1. Particle size characterization of the synthesized silver nanoparticles

Particle size characterization of three types of Ag NPs was performed by using FlFFF as illustrated in Fig. 1. Particle sizes at peaks were 9 nm, 19 nm, and 45 nm for citrate stabilized-Ag NPs, pectin stabilized-Ag NPs, and alginate stabilized-Ag NPs, respectively. The particle size values obtained from FlFFF were in good agreement with those from TEM (Fig. 2) and zetasizer as summarized in Table 3, by which the particle size of alginate stabilized-Ag NPs was larger than pectin stabilized- and citrate stabilized-Ag NPs, respectively.
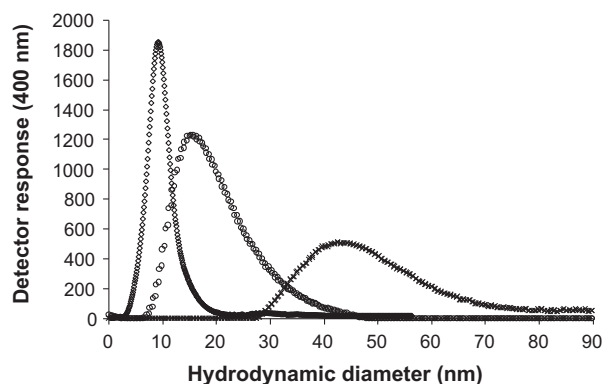

Fig. 1. Hydrodynamic diameter distributions of Ag NPs: (◇) citrate stabilized Ag-NPs; (○) pectin stabilized-Ag NPs; (×) alginate stabilized-Ag NPs. The FlFFF conditions were as follows: channel flow 1 mL min^{-1}, cross flow 1 mL min^{-1}, RC membrane (1 kDa), 0.02% FL-70 and 0.02% NaN$_3$ as carrier liquid. UV–visible was used as FlFFF detector.

Table 3
Particle size of silver nanoparticles (Ag NPs) as determined by various techniques.

Ag NPs	Particle diameter (nm)			
	TEM	Zetasizer	FlFFF with UV–visible[a]	FlFFF with ETAAS[a]
Citrate-stabilized	11.3 ± 3.5	13.6 ± 3.1	9.50 ± 0.0	10.5 ± 0.5
Pectin-stabilized	10.5 ± 5.1	18.3 ± 9.4	19.1 ± 0.1	18.2 ± 0.7
Alginate-stabilized	37.5 ± 2.3	48.8 ± 11	45.5 ± 0.1	40.1 ± 0.4

[a] The mean particle size (d_{mean}) and associated standard deviation ($n = 3$).

With UV–visible absorption spectrometry, the surface plasmon resonance peaks were observed at 390 nm, 400 nm, and 412 nm for citrate stabilized-, pectin stabilized-, and alginate stabilized-Ag NPs, respectively, as shown in Fig. 3, suggesting the same trend as those observed by the FlFFF, TEM, and zetasizer, as the smaller particles exhibit plasmon resonance band as shorter wavelength and the larger particles exhibit the plasmon band at longer wave-
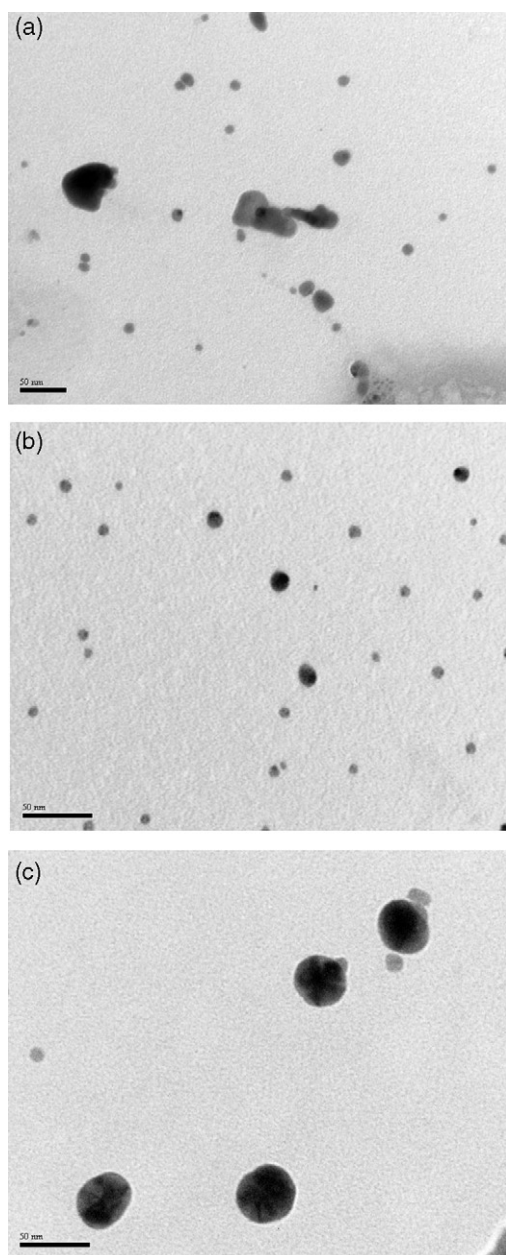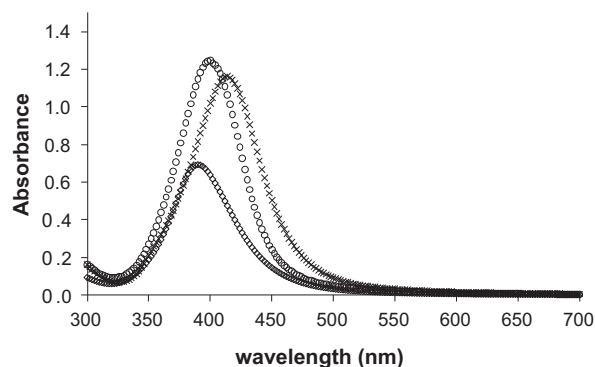

Fig. 3. UV–visible absorption spectra of silver nanoparticles prepared by different stabilizer agents: (◊) citrate stabilized-Ag NPs; (○) pectin stabilized-Ag NPs; (×) alginate stabilized-Ag NPs.

length [17]. Nonetheless, the particle sizes of Ag NPs obtained from different techniques were slightly different owing to the fact that different techniques provide different particle size information. TEM measures a number based size distribution of the core particle excluding the stabilizing agent, while FlFFF and zetasizer measure a mass based size distribution or hydrodynamic volume [13].

3.2. FlFFF with off-line ETAAS detection of silver

Electrothermal atomic absorption spectrometer (ETAAS) was investigated as an off-line detector for FlFFF, as it was previously illustrated possible for SdFFF [18,19]. With the ashing temperature of 800 °C and atomization temperature of 1800 °C for ETAAS determination of silver, it was possible to completely atomize the fractionated particulate sample thus avoiding complex and lengthy sample digestion steps [20]. Nonetheless, to confirm the similarity between the atomization behaviors of the Ag NPs and silver ions, calibration experiments were performed for Ag NPs of various types and silver ions. Calibration curves obtained from all silver types indicate that the slopes were not significantly different, suggesting that the analytical sensitivities were the same for silver of all types. It was 0.0227, 0.0214, 0.0235, and 0.0210 for silver ion, citrate stabilized-, pectin stabilized-, and alginate stabilized-Ag NPs, respectively. The standard t tests with a significance value of 0.05 were performed for data comparison and indicated that the calibration slopes were not significantly different. Table 4 summarizes the characteristic masses, the limits of detection (LOD), and the limits of quantification (LOQ) obtained for silver determination for various

Fig. 2. TEM images of (a) citrate stabilized-Ag NPs, (b) pectin stabilized-Ag NPs, and (c) alginate stabilized-Ag NPs.

Table 4
The characteristic mass (m_o), slope, the limit of detection (LOD) and the limit of quantification (LOQ) for silver determination by ETAAS for various types of Ag NPs and silver ion.

Sample	Slope	m_o (pg)	LOD (µg L^{-1})	LOQ (µg L^{-1})
Ag ion	0.0227	0.8	2.6	8.7
Citrate stabilized-Ag NPs	0.0214	0.9	2.8	9.3
Pectin stabilized-Ag NPs	0.0235	1.0	2.5	8.4
Alginate stabilized-Ag NPs	0.0210	0.9	2.8	9.4

Table 5
The particle size of Ag NPs dispersed in various environmental waters.

Ag NPs	Particle size (nm) of Ag NPs in various types of water as determined by FlFFF-ETAAS		
	Deionized water	Tap water	Ground water
Citrate stabilized	10.5	16.7	n.d.
Pectin stabilized	18.2	19.7	21.2
Alginate stabilized	40.9	40.9	36.7

n.d.: not detectable.

types of silver. As the analytical sensitivities obtained for all types of silver examined in this work were not significantly different, it was possible to use the standard calibration prepared from silver ions for determination of silver in the fractionated silver nanoparticles.

3.3. Ag NPs stability in environmental waters

The stability of Ag NPs in various environmental waters including tap, sea, and ground water was investigated. UV–visible spectrophotometry and FlFFF with ETAAS detection were employed for such investigation. As reported earlier, the shift of the plasmon resonance band of Ag NPs towards the red end or the blue end depends upon the particle size, shape, state of aggregation, and the surrounding dielectric medium [17,21,22]. The blue shift is observed when the particles are smaller, and vice versa the red shift is observed when the particles grow larger. Therefore, UV–visible absorption spectrum can be used to examine the stability and the aggregation behavior of citrate stabilized-Ag NPs, as illustrated in Fig. 4. The maximum absorption of Ag NPs occurred at approximately 400 nm. Upon incubation of Ag NPs in various types of water for 180 min, two bands were observed suggesting that the nanoparticles formed aggregation or deviated from spherical symmetry [17]. Among the three types of Ag NPs synthesized in this study, the stability of alginate stabilized-Ag NPs was higher than that of pectin stabilized- and citrate stabilized-Ag NPs, respectively.

Flow FFF with ETAAS detection was also employed to observe the changes in particle size distribution of various types of Ag NPs upon incubation in various types of water for 180 min as summarized in Table 5. No peak was observed for Ag NPs dispersed in seawater, suggesting that seawater caused change in Ag NPs into free Ag ion or other non-detectable forms. Changes in particle size of Ag NPs were very significant when dispersed in ground water, as compared to those in tap water. In ground water, no peak was observed for citrate stabilized-Ag NPs, whereas it was detectable for other types of Ag NPs, suggesting that the stability of citrate stabilized-Ag NPs was poorer than that of other types of Ag NPs. Fig. 5 illustrates the hydrodynamic diameter distribution of

citrate stabilized-Ag NPs dispersed in various types of water. Further experiments are necessary to investigate parameters affecting changes in particle size of Ag NPs. Tap water was selected to be investigated.

3.4. Parameters affecting particle size of Ag NPs in tap water

In environmental waters, the stability of Ag NPs depends on their surface properties, pH, ionic strength, and the presence of natural organic macromolecules and their concentrations [1,7,13,23]. The stability of the colloidal systems in natural water can be governed by two fundamental mechanisms, which are steric repulsion and charge stabilization or electrostatic interaction [24,25]. The steric repulsion refers to the adsorption of polymers or macromolecules onto the particle surface preventing the particle surfaces coming into close contact with each other. Charge stabilization or electrostatic interaction refers to the distribution of charge species in the system.

For this reason, stabilizing agent was added in the Ag NPs synthesis process to prevent nanoparticles from aggregation and control the particle size of the Ag NPs. Various stabilizing agents, including alginate, citrate, and pectin, were used in the synthesis of Ag NPs. The stability of Ag NPs prepared from different stabilizing agents in environmental waters including tap, sea, and ground water was examined.

3.4.1. Types of stabilizing agent

Ag NPs were dispersed in tap water and UV–visible spectrophotometer was employed to investigate the stability of Ag NPs prepared from various stabilizing agents as shown in Fig. 6. Among the three types of Ag NPs synthesized in this study, the stability of Ag NPs stabilized by alginate was found higher than those stabilized by pectin and citrate, respectively. This information is in good agreement with the zeta potential value (mV) of each Ag NPs as -51.3 ± 1.6, -35.6 ± 2.3 and -34.7 ± 2.4 for alginate, pectin, and citrate stabilized Ag NPs, respectively. The nanoparticles with zeta potential more negative than -30 mV or more positive than
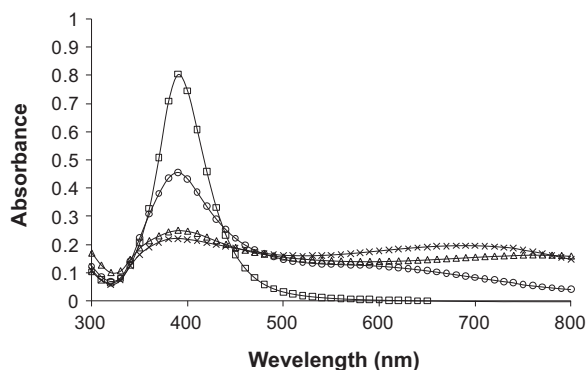

Fig. 4. UV–visible absorption spectra obtained for citrate stabilized-Ag NPs in different types of environmental water: (□) deionized water; (○) tap water; (△) ground water; (×) sea water, at contact time of 180 min.
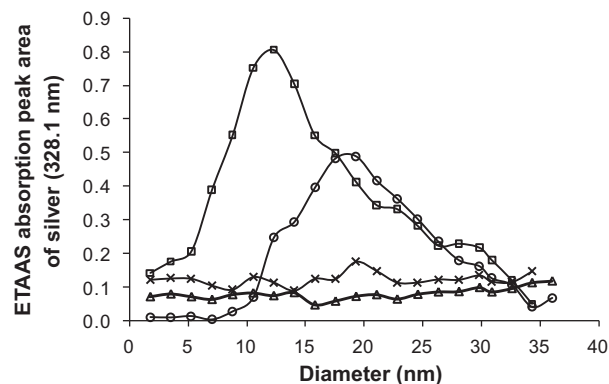

Fig. 5. Hydrodynamic diameter distributions of citrate stabilized-Ag NPs in different types of environmental water: (□) deionized water; (○) tap water; (△) ground water; (×) sea water, at contact time of 180 min. ETAAS was used as FlFFF detector.
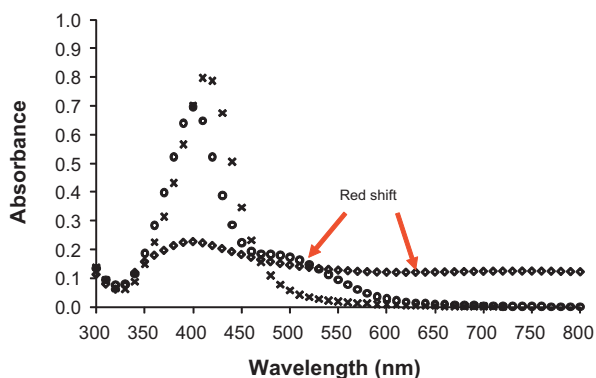
Fig. 6. UV–visible absorption spectra obtained for Ag NPs prepared from different stabilizing agents: (◊) citrate stabilized-Ag NPs; (○) pectin stabilized-Ag NPs; (×) alginate stabilized-Ag NPs in tap water, at contact time of 180 min.

+30 mV are electrically stabilized while nanoparticles with low zeta potentials tend to form aggregates [25].

These findings can be described by steric repulsion. The structure of stabilizing agent is the key factor to control Ag NPs stability; larger steric structure offers higher stability than the smaller steric structure [17]. Therefore, alginate stabilized Ag NPs should have higher stability than pectin and citrate stabilized Ag NPs, respectively, according to the molecular weight of citrate, pectin, and alginate as 258, 30,000–100,000, and 100,000–200,000 g mol^{-1}, respectively.

3.4.2. Effect of contact time

The particle size information obtained from FlFFF with ETAAS detection and zeta potential value from zeta potentiometer were used to provide evidence on Ag NPs aggregation. The aggregation of 20 mg L^{-1} citrate-stabilized Ag NPs in tap water was temporally investigated as demonstrated by shifts in size distributions with increasing contact time. With increasing contact time, the size distributions slightly broadened. The peak maximum appeared at larger diameter size, showing clear evidence of Ag NPs aggregation. The particle size at peak maximum (d_p) and the mean particle size (d_{mean}) increased with increasing contact time (Fig. 7a), suggesting that the aggregation process gradually occurred. The aggregation of Ag NPs was confirmed by zeta potentiometer, and the results are shown in Fig. 7b. The zeta potential values were less negative with increasing contact time, suggesting that the nanoparticles became less stable.

3.4.3. Effect of Ag NPs concentration

The concentration of silver nanoparticles also affects on stability of nanoparticles in water. Therefore, the effect of Ag NPs concentration was examined, as shown in Fig. 8. The mean particle size (d_{mean}) increased when the concentration of Ag NPs decreased. This might be explained by using the DLVO theory, by which the ions present in water cause charge shielding effect, reducing the diffuse layer size and thereby allowing NPs to come into contact sufficiently closely to produce aggregation [26,27]. The very low ion concentrations in tap water were not effective to shield charge of high amount of nanoparticles, but they were sufficient to shield charge of small amount of nanoparticles.

3.4.4. Effect of humic acid

The dissolved organic matter and natural organic macromolecules (NOM) in natural water may react with Ag NPs, which influenced on the stability of Ag NPs. As humic substances are the most important class of NOM in aquatic environment, citrate stabilized-Ag NPs were investigated for their stability in tap water, both in the absence and presence of humic acid using FlFFF with
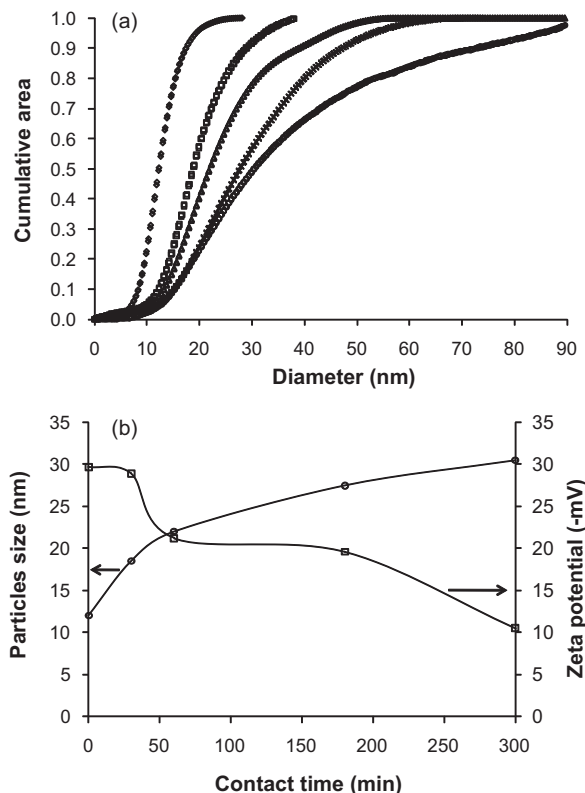

Fig. 7. (a) The cumulative area plot of 20 mg L^{-1} citrate stabilized-Ag NPs in tap water at various contact times: (◊) 0 min; (□) 30 min; (△) 60 min; (×) 180 min; (○) 300 min. (b) Diagram showing the particle size and zeta potential value at various contact times.

ETAAS detection and zeta potential measurement, as illustrated in Figs. 9 and 10, respectively. In the absence of humic acid, the particle sizes of citrate stabilized-Ag NPs increased with longer contact time, as shown in Fig. 9a and the zeta potential values also became less negative with increasing contact time (Fig. 10). In the presence of humic acid of 200 mg L^{-1}, the particle sizes remained unchanged in tap water even at 180 min contact time (Fig. 9b), suggesting that Ag NPs were stabilized with humic acid. This was further confirmed by the observation that the zeta potential values of Ag NPs in the presence of humic acid remained stable with increased contact time, as shown in Fig. 10. These findings are related with the previous reports by Hahn and Stumm [28] who discussed about the effect of NOM to stabilize inorganic colloids in natural waters
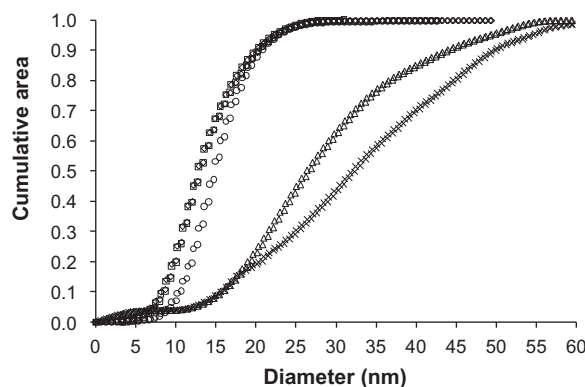

Fig. 8. The cumulative area plot of particle size of citrate stabilized-Ag NPs in tap water at varying concentrations of Ag NPs: (◊) 53 ppm; (□) 40 ppm; (○) 30 ppm; (△) 20 ppm; (×) 10 ppm
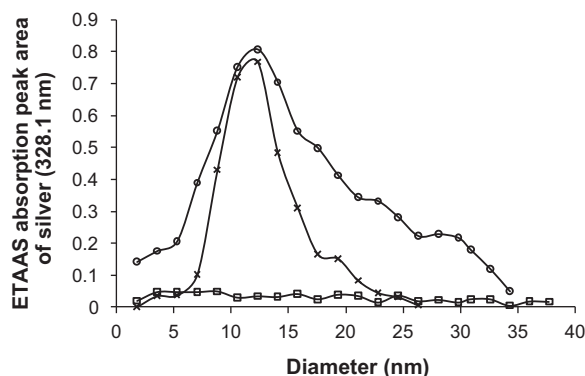
Fig. 9. Particle size distribution of citrate stabilized-Ag NPs: (○) without humic acid in deionized water; (□) without humic acid in tap water; (×) with 200 mg L^{-1} humic acid in tap water, at contact time of 180 min. ETAAS was used as FlFFF detector.
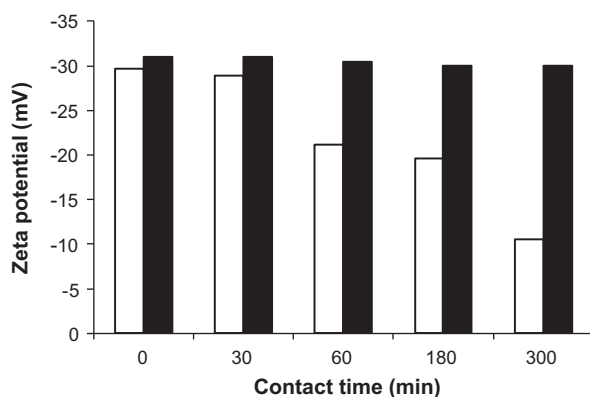

Fig. 10. Zeta potential values of citrate stabilized-Ag NPs in tap water in the absence (□) and presence (■) of 200 mg L^{-1} humic acid.

and Diegoli et al. [17] who reported that humic acid could stabilize the gold colloids in natural waters. Humic acid might cause aggregates to re-disperse or stabilize Ag NPs by steric repulsion [23,29,30].

4. Conclusions

Electrothermal atomic absorption spectrometry (ETAAS) was found efficient as an element specific detector for detection of silver in Ag NPs samples fractionated by FlFFF. In environmental water, citrate stabilized-Ag NPs undergo rapid aggregation than pectin and alginate stabilized-Ag NPs, suggesting that the surface property is the key factor that control the stability of Ag NPs in aquatic system.

Humic acid affects on the stability of Ag NPs in the environment. In summary, the stability of Ag NPs in environmental water depends on the environment conditions such as types of stabilizing agent, contact time, Ag NPs concentration, and the presence of humic acid.

References

[1] S.N. Luoma, PEN Report, Woodrow Wilson International Center for Scholars and The Pew Charitable Trusts, Washington, DC, USA, 2008.
[2] J. Liu, R.H. Hurt, Environ. Sci. Technol. 44 (2010) 2169.
[3] L. Geranio, M. Heuberger, B. Nowack, Environ. Sci. Technol. 43 (2009) 8113.
[4] S.A. Blaser, M. Scheringer, M. MacLeod, K. Hungerbühler, Sci. Total Environ. 390 (2008) 396.
[5] T.M. Benn, P. Westerhoff, Environ. Sci. Technol. 42 (2008) 4133.
[6] O. Choi, Z. Hu, Environ. Sci. Technol. 42 (2008) 4583.
[7] J. Fabrega, S.R. Fawcett, J.C. Renshaw, J.R. Lead, Environ. Sci. Technol. 43 (2009) 7285.
[8] T.M. Tolaymat, A.M. Badawy EI, A. Genaidy, K.G. Scheckel, Sci. Total Environ. 48 (2010) 999.
[9] D.D. Evanoff Jr., G. Chumanov, Chem. Phys. 6 (2005) 1221.
[10] A. Panácek, L. Kvítek, R. Prucek, M. Kolár, R. Vecerova, N. Pizúrová, V.K. Sharma, T. Nevecna, R. Zboril, J. Phys. Chem. B 110 (2006) 16248.
[11] P. Raveendran, J. Fu, S.L. Wallen, J. Am. Chem. Soc. 125 (2003) 13940.
[12] R.F. Domingos, M.A. Baalousha, Y.J. Nam, M.M. Reid, N. Tufenkji, J.R. Lead, G.G. Leppard, K.J. Wilkinson, Environ. Sci. Technol. 43 (2009) 7277.
[13] S.A. Cumberland, J.R. Lead, J. Chromatogr. A 1216 (2009) 9099.
[14] M. Baalousha, J.R. Lead, Sci. Total Environ. 386 (2007) 93.
[15] K. Tiede, A.B.A. Boxall, S.P. Tear, J. Lewis, H. David, M. Hassellöv, Food Addit. Contam. A 25 (2008) 795.
[16] J. Yang, J.Y. Lee, L.X. Chen, H.P. Too, J. Phys. Chem. B 109 (2005) 5468.
[17] S. Diegoli, A.L. Manciulea, S. Begum, I.P. Jones, J.R. Lead, J.A. Preece, Sci. Total Environ. 402 (2008) 51.
[18] G. Blo, A. Ceccarini, C. Conato, C. Contado, F. Fagioli, R. Fuoco, A. Pagnoni, F. Dondi, Anal. Bioanal. Chem. 384 (2006) 922.
[19] C. Contado, G. Blo, F. Fagioli, F. Dondi, R. Beckett, Colloid Surf. A 120 (1997) 47.
[20] P. Liang, L. Peng, Microchim. Acta 168 (2010) 45.
[21] I.E. Sendroiu, S.F.L. Mertens, D.J. Schiffrin, Phys. Chem. Chem. Phys. 8 (2006) 1430.
[22] P. Mulvaney, Langmuir 12 (1996) 788.
[23] E. Navarro, A. Baun, R. Behra, N.B. Hartmann, J. Filser, A.J. Miao, A. Quigg, P.H. Santschi, L. Sigg, Ecotoxicology 17 (2008) 372.
[24] W. Kreyling, M. Semmler-Behnke, W. Möller, J. Nanopart. Res. 8 (2006) 543.
[25] Zeta Potential, An Introduction in 30 Minutes, Zetasizer Nano Series technical note (MRK654-01), Malvern Instruments, Worcestershire, UK, 2006.
[26] H. Christenson, J. Chem. Soc. 80 (1984) 1933.
[27] S. Elzey, V. Grassian, J. Nanopart. Res. 12 (2009) 1945.
[28] W. Stumm, Chemistry of the Solid–Water Interface: Processes at the Mineral-water and Particle-water Interface in Natural Systems, John Wiley & Sons, New York, USA, 1992.
[29] M. Farré, K. Gajda-Schrantz, L. Kantiani, D. Barceló, Anal. Bioanal. Chem. 393 (2009) 81.
[30] J. Buffle, K.J. Wilkinson, S. Stoll, M. Filella, J. Zhang, Environ. Sci. Technol. 32 (1998) 2887.